Aerospace Science and Technology 117 (2021) 106981

Contents lists available at ScienceDirect

Aerospace Science and Technology

www.elsevier.com/locate/aescte

Short communication

Online-learning control with weakened saturation response to attitude tracking: A variable learning intensity approach ☆

Chengxi Zhang [a,*], Choon Ki Ahn [b,*], Jin Wu [c], Wei He [d]

[a] Harbin Institute of Technology, Shenzhen 518055, China
[b] School of Electrical Engineering, Korea University, Seoul 136-701, South Korea
[c] Department of Electronic and Computer Engineering, Hong Kong University of Science and Technology, Hong Kong, China
[d] Institute of Artificial Intelligence, University of Science and Technology Beijing, Beijing 100083, China

ARTICLE INFO

Article history:
Received 18 February 2021
Received in revised form 9 June 2021
Accepted 14 July 2021
Available online 24 July 2021
Communicated by Chaoyong Li

Keywords:
Attitude tracking control
Online-learning control
Variable learning intensity

ABSTRACT

This brief investigates the problem of attitude tracking control using a variable learning intensity (VLI) online-learning control (OLC) scheme. The unique specialty of the proposed VLI-OLC scheme is that it achieves control performance enhancement via learning the previous control information online. The implementation is performed by a simple algebraic equation, which achieves decent control robustness while avoiding a complex control design and saving computational resources. The OLC's saturation response caused by the extensive system error during execution is noticeably weakened by introducing a VLI approach. Compatibility with previous algorithms can be guaranteed. The application example shows that control performance and saturation reduction are guaranteed concurrently.

1. Introduction

1.1. Motivation

Traditional control schemes typically use complex and exquisite structures to improve control performance, robustness, and accuracy. For instance, to achieve control performance enhancement, the commonly used *adaptive tools* [1–5] and *observer tools* [6–9] make the designed algorithms more complicated and necessitate the use of numerous parameters, which increases the controller's conservativeness. However, practical scenarios may not provide all of the ideal conditions required for control systems. In practical spacecraft systems to be in service, there are certain constraints including energy or computational resources. The pressure of launch costs requires designing systems that are simple and efficient to use. This paper aims to design a control scheme with a *simple structure* that consumes *little computational resources* for application in spacecraft attitude control systems.

1.2. Related works

Consider a typical non-linear system

$$\dot{x}(t) = f(t,x) + u(t) + d(t) \tag{1}$$

in which $x(t)$ is the state vector whose domain $D \subset \mathbb{R}^n$ contains the origin; $u(t)$ denotes the control inputs; $d(t)$ denotes the disturbances; $f : [0, +\infty) \times D \to \mathbb{R}^n$ is a piecewise continuous function that has Lipschitz continuity with respect to x. The main task of designing a controller is to investigate an algorithm $u(t)$ that guarantees the stability of the system. To this end, advanced control tools (such as an event-based approach [10,11], prescribed performance approach [3,12,13]; quantization approach [14,15]; and data-driven approach [16]) are utilized while designing the control schemes. Nevertheless, the use of these complex structures in a mathematical operation leads to an increase in the complexity of the algorithm, making it difficult to implement and increasing computational demands.

An effective way to deal with the aforementioned issues is the OLC approach [17], and the control scheme is given by

$$u(t) = k_1 u(t-\tau) + k_2 v \tag{2}$$

where $k_1 u(t-\tau)$ and $k_2 v$ are the learning portion and updating portion, respectively; $\tau > 0$ is the *learning interval*; k_1 and k_2 are positive constants; especially, k_1 is termed as the *learning intensity*, which represents the proportion of previous information utilized

☆ This research is partially supported by the National Natural Science Foundation of China (No. 62003112), the National Research Foundation of Korea (NRF) grant funded by the Korea government (Ministry of Science and ICT) (No. NRF-2020R1A2C1005449), and the Shenzhen Governmental Basic Research Grant (JCY20170412151226061, JCY20170808110410773, JCYJ20180507182241622).

* Corresponding authors.
E-mail addresses: dongfangxy@163.com (C. Zhang), hironaka@korea.ac.kr (C.K. Ahn), jin_wu_uestc@hotmail.com (J. Wu), weihe@ieee.org (W. He).

https://doi.org/10.1016/j.ast.2021.106981
1270-9638/

in generating control instructions; and v is a control law that can stabilize the system dynamics (1). As shown in (2), OLC directly learns the previous control input information via a low-complexity algebraic equation, unlike other traditional algorithms that require analysis of system dynamics or a complex control algorithm design. In this way, though v can be selected using simple designs, control robustness, low computational costs and long-term energy saving can be guaranteed [17].

Nevertheless, the OLC scheme designed in [17] has the following deficiencies. Since the essence of OLC is equivalent to shifting the baseline of the control commands computation, when v is updated to the controller with a large amount (that is, when the system error is large, it will be swiftly learned into the new control commands), the control input u will quickly reach *saturation situation*. The above analysis is verified in [17, Figure 6]. It can be seen from the simulation result that instantaneous energy consumption is excessive at the beginning of the control process due to the short-term saturation. If the aforementioned undesirable property is improved, then the applicability of OLC to practical scenarios will be significantly enhanced. The main obstacles to solve this problem are two twofold.

1) Maintenance of the simple structure and low computational complexity to OLC.
2) Ensuring long-term robustness and decent control performance.

1.3. Contributions

Based on the above analysis and the need to improve OLC, the contributions are threefold.

1) The proposed VLI-OLC design mitigates the noticeable saturation response when encountering a large system error in comparison with [17], without using complex algorithms and introducing many parameters.
2) A satisfactory attitude control performance and high robustness can be guaranteed, including easy parameter tuning, low computational costs, short- and long-term energy-saving, and a weakened saturation response.
3) The proposed VLI-OLC has decent compatibility with conventional control algorithms and can be regarded as a useful extension to improve control performance, as shown from the proof process.

2. Dynamics and problem description

2.1. Attitude dynamics

To begin with, we give the dynamics (3) and kinematics (4), (5) of spacecraft [10]

$$J\dot{\omega} = (J\omega)\times\omega + u + d \tag{3}$$

$$\dot{q} = \frac{1}{2}\left(q^{\times} + q_0 I_3\right)\omega \tag{4}$$

$$\dot{q}_0 = -\frac{1}{2}q^{\top}\omega \tag{5}$$

where $\omega \in \mathbb{R}^3$ denotes the angular velocity of the body-fixed frame ($\mathcal{B}$) with respect to the inertia frame ($\mathcal{I}$) and is expressed in $\mathcal{B}$; $J \in \mathbb{R}^{3\times 3}$ is a symmetric positive-definite matrix which is the inertia dyadic of the body relative to the center of mass resolved in $\mathcal{B}$; $J_{\max}$ and $J_{\min}$ are the maximum and minimum eigenvalues of J; the nominal values of the inertia matrix of the spacecraft can be obtained by referring to [18, Section 4.1]; the cross product of proper vectors a and b can be calculated by $a\times b = -b^{\times}a$ where $b^{\times}$ is a skew-symmetric matrix of b [17]; the unit-quaternion (UQ) approach $Q = \mathrm{col}(q\in\mathbb{R}^3, q_0\in\mathbb{R})$ is utilized to express the attitude of the spacecraft in (4) and (5), describing the orientation of $\mathcal{B}$ with respect to $\mathcal{I}$ and satisfying the UQ operational law $q^{\top}q + q_0^2 = 1$; $I_n \in \mathbb{R}^{n\times n}$ represents the identity matrix; $u\in\mathbb{R}^3$ is the control input provided by actuators; and $d\in\mathbb{R}^3$ represents the exogenous disturbances acting on the systems.

For practical spacecraft attitude control systems, J is a constant matrix, although its specific value may be unknown. The control input capability that the spacecraft actuators can provide is limited, hence the maximum value $u_{\max}$ naturally exists. Moreover, the outer space environment where the spacecraft is located is stable; hence the disturbances it receives mainly come from atmospheric drag, geomagnetic interference, and other factors. Disturbances are usually composed of constant signals, sinusoidal signals with different phases or amplitude, or a combination of both [19–21]. Therefore, d can be assumed to be bounded with $\|d\| \le \bar{d}$.

2.2. Attitude tracking error dynamics

The desired attitude $Q_d = \mathrm{col}(q_d, q_{d0})$ that the spacecraft needs to track can be expressed by the initial attitude Q_{d0} and a desired angular velocity $\omega_d \in \mathbb{R}^3$. Desired signals are designed based on actual missions, and should be bounded, *i.e.*, $\|\omega_d\| \le \alpha_1$ and $\|\dot{\omega}_d\| \le \alpha_2$ with $\alpha_1 > 0$ and $\alpha_2 > 0$. According to the quaternion operational rule, attitude errors $Q_e = \mathrm{col}(q_e, q_{e0})$ can be computed via $q_e = q_{d0}q - (q_d)^{\times}q - q_0 q_d$ and $q_{e0} = (q_d)^{\top}q + q_{d0}q_0$. Besides the constraint $q_e^{\top}q_e + {q_{e0}}^2 = 1$ holds. The spacecraft angular velocity tracking error can be computed via $\omega_e = \omega - C(Q_e)\omega_d$. $C(Q_e)$ is termed as the *rotation matrix* in the form of $C(Q_e) = ({q_{e0}}^2 - q_e^{\top}q_e)I_3 + 2q_e q_e^{\top} - 2q_{e0}{q_e}^{\times}$ and $\|C(Q_e)\| = 1$. The rotation matrix describes the rotation from the desired-frame ($\mathcal{D}$) represented by the desired signal to $\mathcal{B}$. Accordingly, the attitude tracking error dynamics are given by [11]

$$J\dot{\omega}_e = -\omega^{\times}J\omega + J\left(\omega_e^{\times}C(Q_e)\omega_d - C(Q_e)\dot{\omega}_d\right) + u + d \tag{6}$$

$$\dot{q}_e = \frac{1}{2}\left(q_e^{\times} + q_{e0}I_3\right)\omega_e \tag{7}$$

$$\dot{q}_{e0} = -\frac{1}{2}q_e^{\top}\omega_e. \tag{8}$$

Consequently, stabilizing the system's error dynamics (6), (7) and (8) is equivalent to achieving the tracking control of the original system (3), (4) and (5).

2.3. Problem formulation

This paper studies the problem of spacecraft tracking control to a given desired attitude signal. For practical spacecraft, considering the measurement, equipment, and other non-ideal factors, it is unfeasible to expect tracking error to reach zero in real scenarios. We expect the tracking errors to the desired signals to be uniformly ultimately bounded [22, Definition 1] for a given desired signal, *i.e.*:

1) The stability of the system given by (6), (7) and (8) can be guaranteed.
2) $\|Q_e\|$ and $\|\omega_e\|$ converge to small sets containing the origin.

3. Variable learning intensity online-learning control scheme

We first present the VLI-OLC design and introduce its ideas. Subsequently, we provide the proof of attitude tracking stability under the proposed VLI-OLC scheme.

3.1. Control scheme design

The VLI-OLC scheme $u(t) = [u_1, u_2, u_3]^\top$ is designed by

$$u_i(t) = k_{1,i}(t)u_i(t-\tau) + k_2 v_i, \quad i = 1, 2, 3 \tag{9}$$

where the *learning intensity* is defined by

$$k_{1,i}(t) = \exp\left[-\gamma_1 \left(\|u_i(t-\tau)\| + \varepsilon\right)^{\gamma_2}\right] \tag{10}$$

which is a mapping $k_{1,i}(t) : (-\infty, +\infty) \to (0, 1)$; $u(t-\tau)$ denotes the control input information before learning interval τ; $\gamma_1 > 0$, $\gamma_2 > 0$, $\varepsilon > 0$ and $k_2 > 0$ are constants; $v = [v_1, v_2, v_3]^\top = -k_3 \Xi s$ with

$$s = \omega_e + \sigma q_e \tag{11}$$

where $\sigma > 0$, $k_3 > 0$ are constants and $\Xi = \|\omega\|^2 + \|\omega\| + 1$.

Define an aided variable

$$\tilde{u} = u(t) - u(t-\tau) \tag{12}$$

which is termed as *learning difference*. Generally, since actuators have the maximum torque output limit, and the state evolution of actuators, which are usually reaction flywheels, can be assumed to be sufficiently smooth, in relatively short time durations (τ should be selected as a small value), the variation of $u(t)$ can be considered as bounded, *i.e.*, $\|\tilde{u}\| \le \alpha_\tau$ and $\alpha_\tau > 0$. We use the symbol α_τ to represent the maximum learning difference that has a twofold meaning: firstly, $\|\tilde{u}\|$ is assumed bounded; and secondly, the bound α_τ is related to the learning interval τ.

Remark 1. The first item on the right side of the equal sign in (9) represents the controller's learning behavior from the previous control input information when new control instructions are generated. The second item represents the item updated to the control instructions. The learning item has become a sharp difference from the non-learning type control designs.

Remark 2. In comparison with k_1, which is a fixed constant value in [17], in VLI-OLC design, we use a time-varying approach given by (10), which will adjust itself according to the evolution of $u(t-\tau)$. This approach enables the controller to select different learning intensities when the control input is in different situations.

Remark 3. The parameters γ_1, γ_2, and ε in (10) are used to adjust the shape of the mapping $k_1(t)$. γ_1 is used to adjust the learning intensity when $u(t)$ is close to the maximum value; γ_2 is used to adjust the learning intensity when $u(t)$ is close to 0, and ε is a small value to prevent $k_1(t)$ from becoming 1. For practical actuators, the control input limitation $u_{\max}$ exists. Therefore, in this way, it can be guaranteed $0 < \underline{k}_1 = \exp[-\gamma_1(u_{\max} + \varepsilon)^{\gamma_2}] < k_1(t) < \exp(-\gamma_1 \varepsilon^{\gamma_2}) = \bar{k}_1 < 1$ where $\underline{k}_1$ and $\bar{k}_1$ are constants. Note that this is a sufficient condition. The stability of the system in the case of $k_1 = 1$ belongs to a particular algorithm. For example, [23] introduces Assumption A7, but this is an essentially exceptional requirement for the Lyapunov function, making it not as generalizable and compatible as the VLI-OLC algorithm. Hence, it is excluded from the scope of this paper.

Remark 4. τ is the learning interval, and it affects the learning difference $\|\tilde{u}\|$, and subsequently, affects the range of the tracking control convergence region. For common digital control systems, τ can be selected as one or multiple sampling intervals.

Remark 5. As shown in (9), the control law is a simple algebraic equation. In [17], the learning intensity k_1 is a constant. Although it has become a time-varying variable in this design, (10) is a simple and deterministic function. In practical use, techniques such as lookup tables can be used to avoid repeated computations when called. Since it avoids complex adaptive and observer approaches, the proposed VLI-OLC scheme still requires less computation.

Remark 6. The three parameters γ_1, γ_2, and ε together shape the VLI mapping function. By definition, this function is a bell-shaped function. In this function, γ_1 affects the decay rate away from 0, and the larger it is, the faster the function decays; γ_2 determines the degree of flatness of the function near 0, and the larger it is, the flatter the function is in this neighborhood; ε is a constant used to determine the maximum value of $k_1(t)$, and prevent it from equaling 1.

According to (12), it follows that

$$u(t-\tau) = u(t) - \tilde{u}. \tag{13}$$

Substituting (13) into (9) yields $u(t) = k_1(t)(u(t) - \tilde{u}) + k_2 v$ which can be simplified as

$$u(t) = \kappa_1(t)v(t) - \kappa_2(t)\tilde{u} \tag{14}$$

where

$$\kappa_1(t) = \frac{k_2}{1 - k_1(t)}, \quad \kappa_2(t) = \frac{k_1(t)}{1 - k_1(t)}.$$

For convenience, we employ κ_1 and κ_2 for short in the following.

3.2. Stability analysis

Proposition 1. *For spacecraft attitude control system given by (3) - (5) and desired signals, the attitude tracking purpose can be achieved under the utilization of control scheme given by (9) and the final tracking errors are uniformly ultimately bounded, provided the parameters k_1, k_2 and k_3 in (9) - (11) satisfied*

P1) $\beta + (\alpha_\tau - \beta)k_1 < k_2 k_3$;
P2) $(1 - k_1)(\eta_1 + \eta_2) < k_2 k_3$

where β, η_1 and η_2 are positive constants.

Proof of Proposition 1. Select the Lyapunov function $V(t) = 0.5 s^\top J s$. Consider (6) and (7), then the derivative of V is

$$\begin{aligned}
\frac{dV}{dt} &= s^\top J \dot{s} \\
&= s^\top \left(J\dot{\omega}_e + J\sigma \frac{1}{2}\left(q_e^\times + q_{e0} I_3\right)\omega_e \right) \\
&= s^\top \left(\begin{array}{l} -\omega^\times J\omega + J\left(\omega_e^\times C(Q_e)\omega_d - C(Q_e)\dot{\omega}_d\right) \\ + J\sigma \frac{1}{2}\left(q_e^\times + q_{e0} I_3\right)\omega_e + u + d \end{array} \right) \\
&= s^\top \left(L(\cdot) + u \right)
\end{aligned} \tag{15}$$

where

$$\begin{aligned}
L(\cdot) = &- \omega^\times J\omega + J\left(\omega_e^\times C(Q_e)\omega_d - C(Q_e)\dot{\omega}_d\right) \\
&+ J\sigma \frac{1}{2}\left(q_e^\times + q_{e0} I_3\right)\omega_e + d.
\end{aligned} \tag{16}$$

Note that $\omega_e = \omega - C(Q_e)\omega_d$, $\|C(Q_e)\| = 1$, $\|q_e\| < 1$, $\|q_e^\times + q_{e0} I_3\| = 1$, $\|\omega_d\| \le \alpha_1$, $\|\dot{\omega}_d\| \le \alpha_2$ and $\|d\| \le \bar{d}$. According to *Minkowski* and *Hölder* inequalities, we have the following inequalities hold,

$$\begin{aligned}
\|\omega - C(Q_e)\omega_d\| &\le \|\omega\| + \|C(Q_e)\|\|\omega_d\| \le c_1\|\omega\| + c_2\\
\|-\omega^\times J\omega\| &\le \|J\omega\|\|\omega\|\|\sin\angle_{J\omega,\omega}\| \le c_3\|\omega\|^2\\
\|\omega_e^\times C(Q_e)\omega_d\| &\le \|C(Q_e)\|\|\omega_d\|\|\omega_e\|\|\sin\angle_{C(Q_e)\omega_d,\omega_e}\|\\
&\le c_4\|\omega\| + c_5\\
\|C(Q_e)\dot{\omega}_d\| &\le \alpha_2\|C(Q_e)\| \le c_6\\
\|(q_e^\times + q_{e0}I_3)\omega_e\| &\le \|q_e^\times + q_{e0}I_3\|\|\omega_e\| \le c_7\|\omega\| + c_8
\end{aligned} \tag{17}$$

where $c_i > 0, i = 1, 2...8$ are constants. Therefore, it can be concluded that

$$\|L(\cdot)\| \le \beta(\|\omega\|^2 + \|\omega\| + 1) \tag{18}$$

where $\beta \ge \max\{c_3,\ J_{\max}(c_4 + \frac{\sigma}{2}c_7),\ J_{\max}(c_5 + c_6 + \frac{\sigma}{2}c_8) + \bar{d}\}$. Substitute (14) and (18) into (15), then (15) can be re-written as

$$\begin{aligned}
\frac{dV}{dt} &= s^\top (L(\cdot) + u)\\
&= s^\top \left(L(\cdot) + \kappa_1 v(t) - \kappa_2\tilde{u}\right)\\
&= s^\top \left(L(\cdot) - \kappa_1 k_3 s - \kappa_2\tilde{u}\right)\\
&= -\kappa_1 k_3\|s\|^2 + s^\top \left(L(\cdot) - \kappa_2\tilde{u}\right)\\
&\le -\kappa_1 k_3\|s\|^2 + \|s\|\,\|L(\cdot)\| + \alpha_\tau\kappa_2\|s\|\\
&\le -\kappa_1 k_3\Xi\|s\|^2 + \beta\Xi\|s\| + \alpha_\tau\kappa_2\|s\|.
\end{aligned} \tag{19}$$

Next, we discuss two cases.

C1) When $\|s\| > 1$, we have:

$$\begin{aligned}
\frac{dV}{dt} &\le -\kappa_1 k_3\Xi\|s\|^2 + \beta\Xi\|s\| + \alpha_\tau\kappa_2\|s\|\\
&\le -\kappa_1 k_3\Xi\|s\|^2 + \beta\Xi\|s\|^2 + \alpha_\tau\kappa_2\Xi\|s\|^2\\
&= (-\kappa_1 k_3 + \beta + \alpha_\tau\kappa_2)\,\Xi\|s\|^2\\
&\le -\Pi_1
\end{aligned} \tag{20}$$

where $\Pi_1 = \max\{\kappa_1 k_3 - \beta - \alpha_\tau\kappa_2\} > 0$. (20) indicates that if the system's tracking error is large ($\|s\| > 1$), $V(t)$ will decrease at a speed not lower than Π_1 until it reaches $\|s\| = 1$.

C2) When $\|s\| \le 1$:
According to [15, Theorem 2], when s converges to a set containing the origin $\|s\|$, then both $\|\omega_e\|$ and $\|q_e\|$ are bounded. Since $\|\omega_e\|$ is bounded, each dimension of ω_e is bounded. Define the maximum value in all dimensions as ϑ, *i.e.*, $\vartheta = \max\{|\omega_{e,1}|, |\omega_{e,2}|, |\omega_{e,3}|\}$, then $\|\omega\| \le \sqrt{3}\vartheta + \alpha_1$. Therefore, in this case, $\|\Xi\|$ is bounded. Denote $\|\Xi\| \le \xi$, then

$$\begin{aligned}
\frac{dV}{dt} &\le -\kappa_1 k_3\Xi\|s\|^2 + \beta\Xi\|s\| + \alpha_\tau\kappa_2\|s\|\\
&\le -\kappa_1 k_3\|s\|^2 + \beta\xi\|s\| + \alpha_\tau\kappa_2\|s\|.
\end{aligned} \tag{21}$$

Since for arbitrary variables $x \ge 0$ and $y \ge 0$, we have

$$xy \le \eta x^2 + \frac{y^2}{\eta} \tag{22}$$

where $\eta > 0$. Therefore (21) can be expressed as

$$\begin{aligned}
\frac{dV}{dt} &\le -\kappa_1 k_3\Xi\|s\|^2 + \beta\Xi\|s\| + \alpha_\tau\kappa_2\|s\|\\
&\le -\kappa_1 k_3\|s\|^2 + \beta\xi\|s\| + \alpha_\tau\kappa_2\|s\|\\
&\le -\kappa_1 k_3\|s\|^2 + \eta_1\|s\|^2 + \frac{(\beta\xi)^2}{\eta_1} + \eta_2\|s\|^2\\
&\quad + \frac{(\alpha_\tau\kappa_{2,\max})^2}{\eta_2}\\
&= (-\kappa_1 k_3 + \eta_1 + \eta_2)\,\|s\|^2 + \frac{(\beta\xi)^2}{\eta_1} + \frac{(\alpha_\tau\kappa_{2,\max})^2}{\eta_2}\\
&\le -\Pi_2 V + \delta
\end{aligned} \tag{23}$$

where $\eta_1 > 0$, $\eta_2 > 0$, $\Pi_2 = \max\{\frac{2(\kappa_1 k_3 - \eta_1 - \eta_2)}{J_{\max}}\} > 0$, and $\delta = \frac{(\beta\xi)^2}{\eta_1} + \frac{(\alpha_\tau\kappa_{2,\max})^2}{\eta_2}$. According to [22, Definition 1], s will be uniformly ultimately bounded, besides satisfying the following inequality

$$s^\top(t) J s(t) \le e^{-(K_2 t)} s^\top(0) J s(0) + \frac{\delta}{\Pi_2}, \tag{24}$$

namely, the ball is

$$\limsup_{t\to\infty}\|s(t)\| \le \sqrt{\frac{\delta}{\Pi_2 J_{\min}}}. \tag{25}$$

Reuse [15, Theorem 2], it can be concluded that both $\|\omega_e\|$ and $\|q_e\|$ are uniformly ultimately bounded.

Consequently, the behavior of the system can be concluded as follows. First, the system energy function will converge to $\|s\| = 1$ at the rate of no less than Π_1, and then asymptotically converge to a small region.

Therefore, this completes the proof. □

4. Comparative simulations

4.1. Parameter configuration

To test the robustness of the VLI-OLC algorithm, the uncertainty of inertia is also considered in the simulation.

- Denote $J = \bar{J} + \Delta J$ (kg·m^2) in (3) where
  Nominal value [24] $\bar{J} = \begin{bmatrix} 20 & 2 & 0.9 \\ 2 & 17 & 0.5 \\ 0.9 & 0.5 & 15 \end{bmatrix}$,
  Inertia uncertainty $\Delta J = \text{diag}\begin{pmatrix} (3+\sin(0.5t))e^{-0.1t} + 1 \\ (4+\cos(0.5t))e^{-0.1t} + 2 \\ (5+\sin(0.5t))e^{-0.1t} - 1 \end{pmatrix}$;
- Disturbance [25] $d(t) = \begin{bmatrix} -3\cos(\phi t) - 6\sin(0.3\phi t) + 3 \\ 1.5\sin(\phi t) - 3\cos(0.5\phi t) - 2 \\ -3\sin(\phi t) + 8\sin(0.4\phi t) - 1 \end{bmatrix} 10^{-3}$ (N·m) where $\phi = 0.5 + \|\omega\|$, in (3);
- Controller $u(t)$ parameters, $\gamma_1 = 4$, $\gamma_2 = 2$, $\varepsilon = 0.1$, $k_2 = 1$, $k_3 = 2$, $\sigma = 1$, in (9), (10), (11);
- Desired signal (rad/s) in (6)
  $\omega_d(t) = 10^{-2}[\cos(\psi), -\sin(\psi), -\cos(\psi)]^\top$ with $\psi = 0.1t$;
- Initial value $\omega(0) = [0, 0, 0]^\top$ in (3),
  $Q(0) = [(-0.2, 0.3, -0.2), \sqrt{0.83}]^\top$ in (4).

To better verify the control algorithm's performance in practical scenarios, an actuator model that considers multiple non-ideal factors for simulation is utilized in this simulation, including second-order dynamics [26], dead zone, bias torque, saturation, time-delay, and health-index [20]. Moreover, the actuator parameter settings mentioned above are the same as that in [11, Table II], which are given by: time-delay ($t_d = 0.01$ s), second-order dynamics ($T_u = 0.03$, $T_v = 0.03$), bias torque ($\tau_0 = 0.001$ N·m), dead zones (up=−0.001 N·m, low=0.001 N·m), health index (95%), saturation (up=1 N·m, low=-1 N·m). Moreover, to exhibit the actuator's

energy consumption characteristic of the proposed control algorithm, we use the arrangement in [17], defining the energy index $E = [E_x, E_y, E_z]^\top$ where

$$E_i = \frac{P_i}{P_{i,\text{Non-OLC}}},\ P_i = \int |u_i| dt,\ i = x, y, z. \tag{26}$$

Eq. (26) indicates that we use the compared Non-OLC algorithm energy consumption as a baseline. $E_i = 1$ means the consumption is roughly the same. $E_i > 1$ indicates that the proposed algorithm's energy consumption is relatively large, and vice versa.

Remark 7. There are two aspects of the VLI-OLC algorithm that must be considered for parameter tuning in simulation. The first is to tune parameter $k_1(t)$. ε determines the maximum value of $k_1(t)$, which regulates the control accuracy. Generally, we make ε small to improve the tracking accuracy. Moreover, γ_1 and γ_2 determine the degree of $k_1(t)$ decay when the control input is large. The meanings of each parameter are introduced in Remark 6. The second is to tune parameter k_2. It should be noted that k_2 shares the same role as k_3 in v. They must satisfy P1 and P2 conditions in Proposition 1. From a convenience perspective, if v is a controller that can stabilize the system, then k_2 can be tuned starting from 1.

Remark 8. The two conditions (P1, P2) in Proposition 1 are easy to meet. Although they are two conditions, the selection of parameters is not mutually constraining. From the previous analysis, we can know

- There exist upper and lower bounds for $k_1(t)$, *i.e.*, $0 < \underline{k}_1 < k_1(t) < \bar{k}_1 < 1$.
- Consider the definition of learning difference. In fact, α_τ is small and tends to 0; *i.e.*, $\alpha_\tau \to 0$.
- η_1 and η_2 affect the size of the ball converged to, but are positive enough to satisfy the requirement.

Based on the above analysis, we use a conservative way to simplify P1, P2 to obtain P1:$\beta(1-\underline{k}_1) + \alpha_\tau \bar{k}_1 < k_2 k_3 \Rightarrow \beta + \alpha_\tau < k_2 k_3$; P2:$(1-\underline{k}_1)(\eta_{1\min} + \eta_{2\min}) < k_2 k_3 \Rightarrow \eta_{1\min} + \eta_{2\min} < k_2 k_3$. Hence, we get $\max\{\beta + \alpha_\tau, \eta_{1\min} + \eta_{2\min}\} < k_2 k_3$. If we choose a small learning interval and let $\eta_{1\min} + \eta_{2\min} = 1$, the result can further be $\max\{\beta, 1\} < k_2 k_3$. Moreover, β can be obtained empirically in engineering; for example, a similar estimate of b (β herein) in [27, Eq. (19) and Fig. 10] results in $\hat{b} < 0.03$. The above more conservative conclusion shows that the requirement is easily guaranteed as long as we select a large value for $k_2 k_3$.

4.2. Simulation results

In this simulation, we test the proposed control algorithm and compare it with two other algorithms to show the performance. We use the abbreviation VLI-OLC to denote the proposed variable learning intensity online learning control scheme; OLC to denote the control scheme in [17] where the learning intensity is a constant value $k_1 = 0.9$; and Non-OLC to denote the case where the learning mechanism is not used, *i.e.*, without the learning item in (9).

Figs. 1 - 5 provide the simulation results. Figs. 1 and 2 display the angular velocity and attitude tracking error to the desired signals (to make the data more intuitive, we converted the UQ description into rotation angles (RA) using the ZYX order). It can be seen from the figure that after about 50 s from the start of the simulation, three control algorithms have entered a stable tracking state. However, the zoomed-in state can be seen on the right side

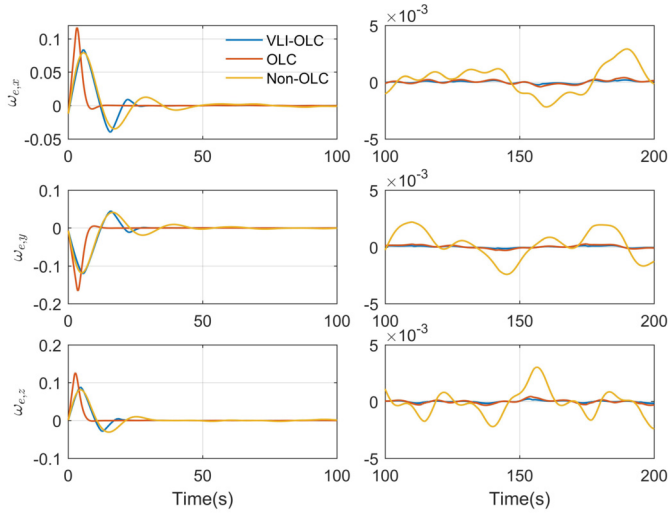

Fig. 1. Evolution of angular velocity error.

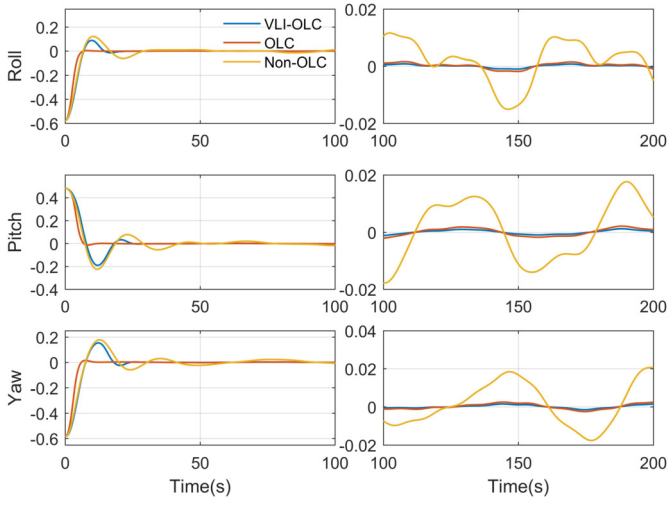

Fig. 2. Evolution of attitude tracking error.

of the figure that the tracking errors are different. The control performance that uses the learning mechanism is better than that of non-OLC. The VLI-OLC performance is in the same order of magnitude as the fixed learning intensity OLC. Moreover, the tracking accuracy of the VLI-type is increased by over 20% in this simulation compared to the fixed-type (see Table 1). Fig. 3 shows the control input response of three actuators. As can be seen, the cost of Non-OLC not making the controller saturated is at the expense of tracking accuracy. The OLC brings high-precision control effects, but saturation occurs at the initial stage of large errors due to the fixed learning intensity. Additionally, VLI-OLC produces a control torque that is significantly away from the saturation value while maintaining the satisfactory control accuracy of OLC. It is worth noting that the VLI-OLC provides a slower convergence speed than the OLC. Since no change in performance can be cost-free, to some extent, it is indeed a trade-off, but it is actually more than that. The innovative change is simple, easy to implement, and practical to real scenarios, enabling the actuator to avoid excessive torque as much as possible, as we would expect. Fig. 4 shows the inertia uncertainty, disturbance, and shifts in learning intensity used in this simulation. In the third portion of Fig. 4, the curves' evolution shows why the saturation in Fig. 3 is avoided: as the control torque increases, the learning intensity will be reduced. Fig. 5 shows a comparison of energy indices. The following threefold points of

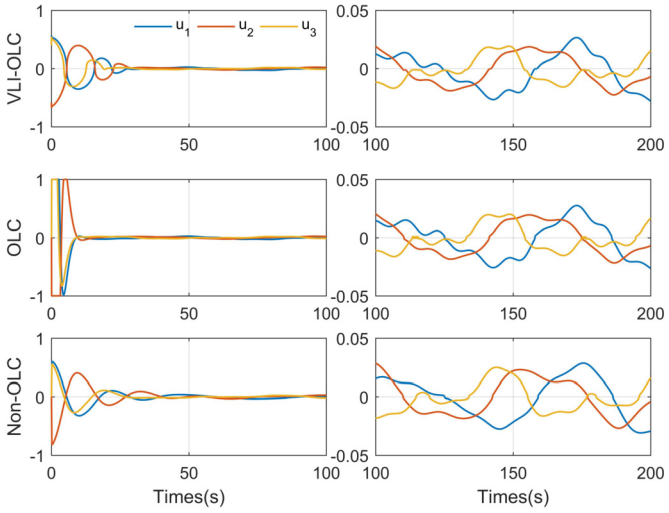

Fig. 3. Control torques acting on actuator with dynamics.

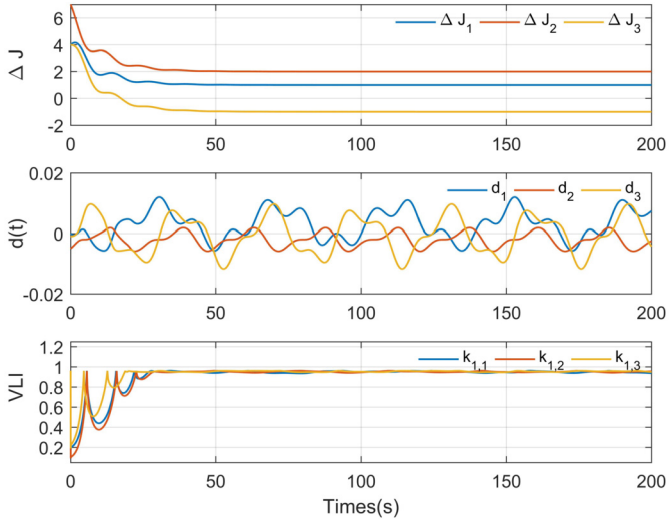

Fig. 4. Inertia uncertainty, disturbance and variable learning intensity.

Table 1
Simulation result summary.

Item	VLI-OLC	OLC	Non-OLC
ω_e (rad/s)	$< 3 \times 10^{-4}$	$< 4 \times 10^{-4}$	$< 3 \times 10^{-3}$
q_e (rad)	$< 2 \times 10^{-3}$	$< 3 \times 10^{-3}$	$< 2 \times 10^{-2}$
E	< 1	< 1	1

information can be noticed: 1. Both OLC schemes consume more energy in the short term than Non-OLC. 2. After about 700 s, the energy index of both dropped below one, indicating that long-term energy-saving can be achieved. 3. VLI-OLC reduces the saturation response and saves energy more than OLC.

The data in Table 1 present a summary of the simulation results. Generally speaking, the control accuracy of VLI-OLC is at the same level as OLC. In the long term, VLI-OLC is also more energy-efficient than OLC. As shown in Figs. 1-3 and Table 1, there are more opportunities to tune the control process when using the VLI approach while also ensuring control accuracy. Therefore, the trade-off is worth it. The proposed VLI-OLC addresses the problem of OLC becoming saturated and further advances this approach.

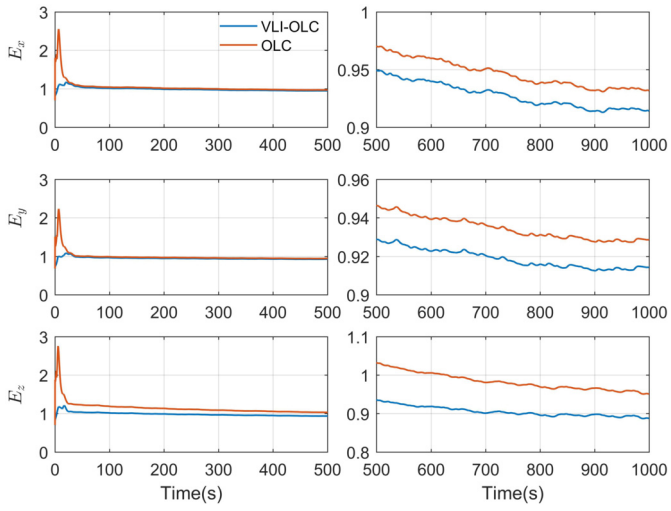

Fig. 5. Relative energy consumption index comparison.

5. Conclusions

In this paper, a novel variable learning intensity online learning control scheme is proposed to achieve attitude tracking control. The most significant nature of VLI-OLC is that it inherits OLC's excellent control performance properties, with a high control accuracy and a low-complexity structure, avoiding the usage of complex tools such as adaptive and observers. Specifically, by introducing a novel VLI approach, the proposed VLI-OLC efficiently reduces the saturation induced by large tracking errors. The advantages of the algorithm are verified through comparison simulations that are subjected to various internal and external disturbances; VLI-OLC can achieve the control object favorably. In the future, we will further focus on the discussion of the prescribed performance control characteristics of the OLC algorithm.

Declaration of competing interest

The authors declare that they have no known competing financial interests or personal relationships that could have appeared to influence the work reported in this paper.

References

[1] Z. Liu, Z. Han, Z. Zhao, W. He, Modeling and adaptive control for a spatial flexible spacecraft with unknown actuator failures, Sci. China Inf. Sci. 64 (5) (2021) 1–16.
[2] S.-K. Kim, J.K. Park, C.K. Ahn, Learning and adaptation-based position-tracking controller for rover vehicle applications considering actuator dynamics, IEEE Trans. Ind. Electron. (2021) 1, https://doi.org/10.1109/TIE.2021.3065604.
[3] C. Wei, J. Luo, B. Gong, M. Wang, J. Yuan, On novel adaptive saturated deployment control of tethered satellite system with guaranteed output tracking prescribed performance, Aerosp. Sci. Technol. 75 (2018) 58–73, https://doi.org/10.1016/j.ast.2018.01.014.
[4] C. Zhang, M.-Z. Dai, J. Wu, B. Xiao, B. Li, M. Wang, Neural-networks and event-based fault-tolerant control for spacecraft attitude stabilization, Aerosp. Sci. Technol. 114 (2021) 106746, https://doi.org/10.1016/j.ast.2021.106746.
[5] C. Zhang, J. Wang, D. Zhang, X. Shao, Fault-tolerant adaptive finite-time attitude synchronization and tracking control for multi-spacecraft formation, Aerosp. Sci. Technol. 73 (2018) 197–209, https://doi.org/10.1016/j.ast.2017.12.004.
[6] X. Zhu, J. Chen, Z.H. Zhu, Adaptive learning observer for spacecraft attitude control with actuator fault, Aerosp. Sci. Technol. 108 (2021) 106389, https://doi.org/10.1016/j.ast.2020.106389.
[7] C. Wu, J. Yan, H. Lin, X. Wu, B. Xiao, Fixed-time disturbance observer-based chattering-free sliding mode attitude tracking control of aircraft with sensor noises, Aerosp. Sci. Technol. 111 (2021) 106565, https://doi.org/10.1016/j.ast.2021.106565.
[8] X.G. Guo, M.E. Tian, Q. Li, C.K. Ahn, Y.H. Yang, Multiple-fault diagnosis for spacecraft attitude control systems using RBFNN-based observers, Aerosp. Sci. Technol. 106 (2020) 106195, https://doi.org/10.1016/j.ast.2020.106195.

[9] S.K. Kim, C.K. Ahn, Learning algorithm-based offset-free one-step time-delay compensation for power converter and motor drive system applications, IEEE Trans. Ind. Inform. 16 (6) (2020) 3789–3796, https://doi.org/10.1109/TII.2019.2939656.
[10] C. Zhang, M.-Z. Dai, P. Dong, H. Leung, J. Wang, Fault-tolerant attitude stabilization for spacecraft with low-frequency actuator updates: an integral-type event-triggered approach, IEEE Trans. Aerosp. Electron. Syst. 57 (1) (2021) 729–737, https://doi.org/10.1109/TAES.2020.3009542.
[11] C. Zhang, C.K. Ahn, B. Xiao, J. Wu, On attitude tracking control with communication-saving: an integrated quantized and event-based scheme, IEEE Trans. Circuits Syst. II, Express Briefs (2021), https://doi.org/10.1109/TCSII.2020.3047679.
[12] J. Luo, Z. Yin, C. Wei, J. Yuan, Low-complexity prescribed performance control for spacecraft attitude stabilization and tracking, Aerosp. Sci. Technol. 74 (2018) 173–183, https://doi.org/10.1016/j.ast.2018.01.002.
[13] C. Zhang, J. Wu, C.K. Ahn, Z. Fei, C. Wei, Learning observer and performance tuning based robust consensus policy for multi-agent systems, IEEE Syst. J. (2021), https://doi.org/10.1109/JSYST.2020.3047644.
[14] R. Sun, A. Shan, C. Zhang, J. Wu, Q. Jia, Quantized fault-tolerant control for attitude stabilization with fixed-time disturbance observer, J. Guid. Control Dyn. 44 (2) (2021) 449–455, https://doi.org/10.2514/1.G005465.
[15] B. Wu, Spacecraft attitude control with input quantization, J. Guid. Control Dyn. 39 (1) (2016) 1–5, https://doi.org/10.2514/1.G001427.
[16] Y. Jiang, J.L. Fan, W.N. Gao, T.Y. Chai, F.L. Lewis, Cooperative adaptive optimal output regulation of discrete-time nonlinear multi-agent systems, Automatica 121 (2020) 109149, https://doi.org/10.1016/j.automatica.2020.109149.
[17] C. Zhang, B. Xiao, J. Wu, B. Li, On low-complexity control design to spacecraft attitude stabilization: an online-learning approach, Aerosp. Sci. Technol. 110 (2021) 106441, https://doi.org/10.1016/j.ast.2020.106441.
[18] M.J. Sidi, Spacecraft Dynamics and Control: A Practical Engineering Approach, vol. 7, Cambridge University Press, 1997.
[19] A. Sanyal, A. Arbor, Inertia-free spacecraft attitude tracking with disturbance rejection and almost global stabilization, J. Guid. Control Dyn. 32 (4) (2009), https://doi.org/10.2514/1.41565.
[20] C. Zhang, J. Wu, R. Sun, M. Wang, D. Ran, Actuator model for spacecraft attitude control simulation, Aircr. Eng. Aerosp. Technol. (2021), https://doi.org/10.1108/AEAT-10-2020-0226.
[21] Q. Shen, D. Wang, S. Zhu, E.K. Poh, Robust control allocation for spacecraft attitude tracking under actuator faults, IEEE Trans. Control Syst. Technol. 25 (3) (2017) 1068–1075, https://doi.org/10.1109/TCST.2016.2574763.
[22] Y. Lee, S.H. Zak, Uniformly ultimately bounded fuzzy adaptive tracking controllers for uncertain systems, IEEE Trans. Fuzzy Syst. 12 (6) (2004) 797–811, https://doi.org/10.1109/TFUZZ.2004.836087.
[23] W. Chen, M. Saif, An iterative learning observer-based approach to fault detection and accommodation in nonlinear systems, in: Proc. 40th lEEE Conf. Decis. Control, Orlando, USA, 2001, pp. 4469–4474.
[24] J.D. Boškovic, S.-M. Li, R.K. Mehra, Robust adaptive variable structure control of spacecraft under control input saturation, J. Guid. Control Dyn. 24 (1) (2001) 14–22, https://doi.org/10.2514/2.4704.
[25] B. Li, Q. Hu, Y. Yang, Continuous finite-time extended state observer based fault tolerant control for attitude stabilization, Aerosp. Sci. Technol. 84 (2019) 204–213, https://doi.org/10.1016/j.ast.2018.10.006.
[26] R. Kristiansen, D. Hagen, Modelling of actuator dynamics for spacecraft attitude control, J. Guid. Control Dyn. 32 (3) (2009) 1022–1025, https://doi.org/10.2514/1.42574.
[27] B. Wu, X. Cao, Robust attitude tracking control for spacecraft with quantized torques, IEEE Trans. Aerosp. Electron. Syst. 54 (2) (2018) 1020–1028, https://doi.org/10.1109/TAES.2017.2773273.